

Analytic modeling of the conductance in quantum point contacts with large bias

T. Ouchterlony and K.-F. Berggren

Department of Physics and Measurement Technology, Linköping University, S-581 83 Linköping, Sweden

(Received 27 June 1995)

We have developed a model for calculating differential conductance that accounts for the effects observed at high source-drain voltage. The model uses a linear potential drop over a saddle-point potential. If the region of the potential drop is wide enough, only that region is contributing to the transmission and a simple expression is obtained. The temperature is assumed to increase linearly with the source-drain voltage and a model for an equipotential region in the saddle-point potential corresponding to the channel width is made. The result from the calculations of the conductance with this model is in good agreement with experimental results.

I. INTRODUCTION

The subject of quantum point contacts has been of considerable interest in many varying aspects,¹⁻⁹ both theoretically and experimentally. When the size of a semiconductor structure is of the same scale as the electron wavelength, the behavior of the electrons is governed by quantum mechanics. The construction of such devices has been possible thanks to a recent technological development.¹⁰ In a narrow constriction in a two-dimensional electron gas the electron transport is ballistic, i.e., the electrons move freely in the longitudinal direction and are quantized in the transverse directions. The conductance of such a quasi-one-dimensional constriction is quantized in units of $2e^2/h$, which was discovered experimentally by two groups in 1988.^{1,2} The quantization holds at low temperatures and when the potential drop applied over the constriction is small. If the bias voltage is increased half-plateaus occur between the multiples of $2e^2/h$.³ At high voltage the half-plateaus are blurred.⁴

The purpose of this paper is to propose a model that accounts for the high-bias region. This is done in Secs. II-VI. In Sec. VII we compare the theory with recent experiments.

II. THEORY

An analytical model for a narrow constriction was applied by Büttiker,¹¹ using a saddle-point potential

$$V(x,y) = V_0 - \frac{1}{2}m^* \omega_x^2 x^2 + \frac{1}{2}m^* \omega_y^2 y^2. \tag{1}$$

This kind of potential was used in calculation of tunneling in nuclear physics already in 1953.^{12,13} The transmission through this potential is for each channel $T_n = 1/(1 + e^{-\pi\epsilon_n})$ when no potential drop V_{sd} is applied between source and drain. Here $\epsilon_n = 2[E - E_n - V_0]/\hbar\omega_x$, and $E_n = \hbar\omega_y(n + \frac{1}{2})$ is the harmonic-oscillator energy levels. This expression for the transmission has also been used as an approximation for small nonzero V_{sd} . The main reasons for this are that the saddle-point potential is analytically solvable and that accurate quantitative results can be achieved.⁴

The general expression for the current through a potential barrier with total transmission $T(E, V_{sd})$ is

$$I = \frac{2e}{h} \int_{-\infty}^{\infty} dE T(E, V_{sd}) \times \{f_s(E - \beta eV_{sd}) - f_d[E + (1 - \beta)eV_{sd}]\}, \tag{2}$$

where β is the fraction of the potential that drops on the source side (see Fig. 1) and f_s and f_d are Fermi functions,

$$f(E) = \frac{1}{e^{(E - \mu)/k_B T} + 1}, \tag{3}$$

on the source and drain sides, respectively. Here μ is the chemical potential, k_B Boltzmann's constant, and T the temperature. The differential conductance is

$$G = \frac{\partial I}{\partial V_{sd}}. \tag{4}$$

The conductance for zero temperature is then given by

$$G = \frac{\partial}{\partial V_{sd}} \left[\frac{2e}{h} \int_{E_F - (1 - \beta)eV_{sd}}^{E_F + \beta eV_{sd}} dE T(E, V_{sd}) \right]. \tag{5}$$

For the saddle-point potential in Eq. (1) we have

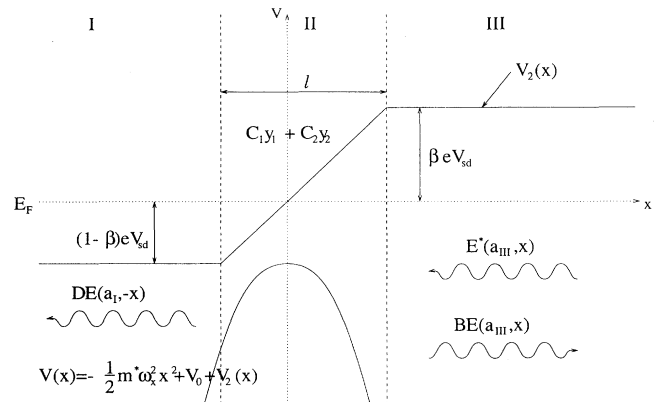


FIG. 1. The linear potential drop over the saddle point. β is the ratio of the potential drop on the right side of the saddle point, y_1 and y_2 are power series solutions of Eq. (8), $E(a, x)$ parabolic cylinder function solutions, and B, C_1, C_2 , and D are complex constants to be determined.

$$T(E, V_{sd}) = \sum_n T_n(E, V_{sd}) = \sum_n \frac{1}{1 + e^{-\pi\epsilon_n}}, \quad (6)$$

which is independent of V_{sd} . Thus the conductance is

$$G = \frac{2e^2}{h} \sum_n \{ \beta T_n(E_F + \beta e V_{sd}) + (1 - \beta) T_n[E_F - (1 - \beta)e V_{sd}] \}. \quad (7)$$

This expression is in very good agreement with experiment at low bias V_{sd} , but when the bias is increased it differs substantially from the experimental results (see, e.g., Frost *et al.*⁴).

III. MODEL OF LINEAR POTENTIAL DROP

In this paper a linear potential drop¹⁴ over the saddle-point is introduced explicitly (Fig. 1). We make this choice because it is more realistic than just assuming that the potential is higher on one side of the saddle point than on the other as in Frost *et al.*,⁴ and Martin-Moreno *et al.*³ In addition, the mathematical properties are appealing. This leads to equations of the same type as for an unbiased saddle-point potential,

$$\frac{d^2 y}{dx^2} + (\frac{1}{4}x^2 - a)y = 0. \quad (8)$$

In this case a is different in the three regions. This equation is analytically solvable in each region and the constants are determined by matching the wave functions and their derivatives at the boundaries. It has also other useful analytical properties. The equality for the parabolic cylinder function solutions,¹⁵

$$\sqrt{1 + e^{2\pi a}} E(a, x) = e^{\pi a} E^*(a, x) + i E^*(a, -x), \quad (9)$$

leads directly to the transmission T_n above. Also, the Wronskian

$$W\{E(a, x), E^*(a, x)\} = -2i \quad (10)$$

has a simple form, and makes the evaluation of the current straightforward.

The procedure outlined above works well for not too high bias. For high bias, however, the matching process becomes numerically unstable. Fortunately, a reliable approximation, which is examined below, can be made.

IV. APPROXIMATION FOR WIDE REGION OF POTENTIAL DROP

The important region for the transmission is where the potential reaches its maximum value. If the potential drop is assumed to be over a wide region, this value is well inside region II in Fig. 1. As an approximation this region may be extended to the whole x axis (Fig. 2). For this approximation the transmission can be calculated analytically, and the result differs from the unbiased saddle-point potential only in an extra term in the exponent depending on V_{sd} ,

$$T_n = \frac{1}{1 + e^{-2\pi[E - E_n - V_0 - (1/2)\alpha e V_{sd}]/\hbar\omega_x}}, \quad (11)$$

where

$$\alpha = \frac{e V_{sd}}{l^2 m^* \omega_x^2}. \quad (12)$$

We insert the transmission in Eq. (2), and apply Eq. (4) to get

$$G = \frac{2e^2}{h} \int_{-\infty}^{\infty} dE T(E, V_{sd}) \times \left\{ \left[\beta - \alpha \right] \left[-\frac{\partial f_s}{\partial E} \right] + \left[1 - \left[\beta - \alpha \right] \right] \left[-\frac{\partial f_d}{\partial E} \right] \right\}. \quad (13)$$

For zero temperature the expression of the conductance simplifies to

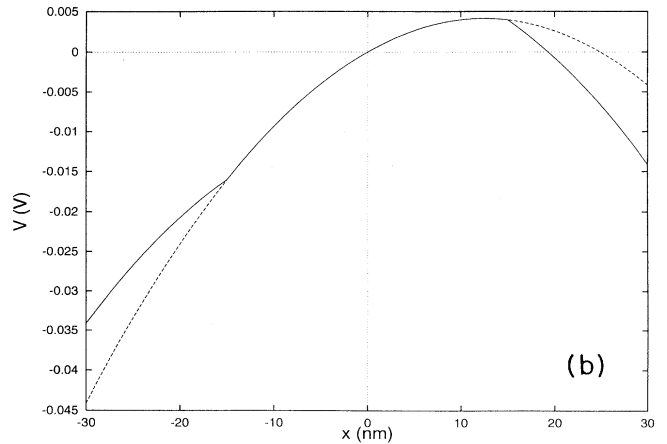
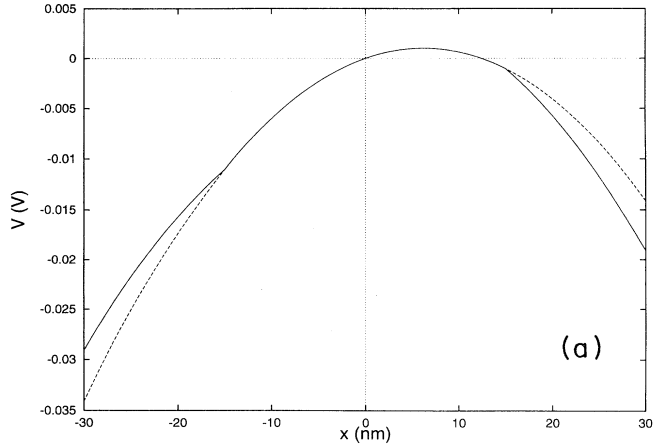


FIG. 2. The total potential for the full model of a linear potential drop (line) and the approximation (broken line) when $l = 30$ nm, $\beta = 0.5$, $m^* = 0.2m_e$, and $\hbar\omega_x = 4.5$ meV. V_{sd} is in (a) 10 mV where the maximum of the potential is far from the edge of the middle region, and in (b) 20 mV where the maximum is near the edge and the approximation is not valid.

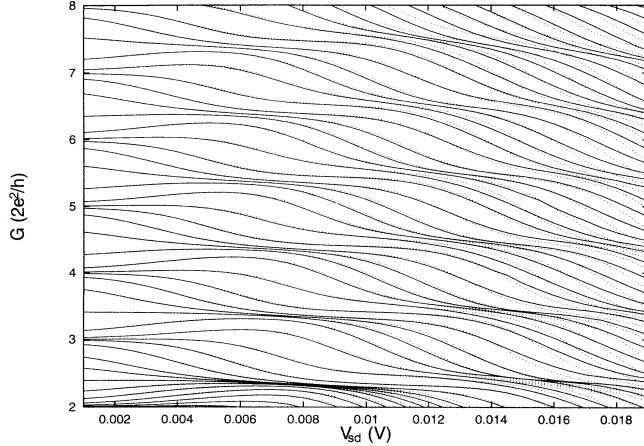


FIG. 3. Conductance for the full model (line) and the approximation (dots) with $l=30$ nm, $\beta=0.5$, $m^*=0.2m_e$, $\hbar\omega_x=4.5$ meV, $\hbar\omega_y=9.0$ meV, and $T=0$ K. A few points in the full model are misplaced due to numerical instability.

$$G = \frac{2e^2}{h} \sum_n \{ (\beta - \alpha) T_n(E_F + \beta e V_{sd}, V_{sd}) + [1 - (\beta - \alpha)] T_n[(E_F - (1 - \beta)e V_{sd}, V_{sd})] \}. \quad (14)$$

This equation is very similar to Eq. (7). Introducing a dependence of V_{sd} in this way simply corresponds to a shift in the coefficient β and in a change in the transmission.

A comparison between the conductance in the full model, and the approximation for a wide potential drop is given in Fig. 3. Below 10 mV the approximation is obviously fair. It fails for larger V_{sd} when the hump in the potential is closer to the edge of the linear slope region (compare with Fig. 2).

V. THE TEMPERATURE VARIATION

For small applied voltages the temperature in the quantum point contact is equal to the temperature of the surrounding bath. When the voltage is increased, the increasing current induces heat, and the temperature is raised. According to Taboryski *et al.*,¹⁶ the effective temperature T in the quantum point contact is calculated from the bath temperature T_0 , the current I , and the number of occupied levels n , through

$$k_B T = \sqrt{(k_B T_0)^2 + CI^2/n^2}, \quad (15)$$

where C is a fitting parameter. T_0 is negligible for high voltages, and for small voltages the temperature T is so small that it has no effect on the conductance. The number of occupied levels is approximately proportional to the conductance, which in turn is approximately proportional to I/V_{sd} . This results in

$$T \propto V_{sd}. \quad (16)$$

Introducing temperature in the model will decrease the

conductance for high temperatures, i.e., high applied voltages.

VI. THE WIDTH OF THE CHANNEL

Experimentally it has been found that for increasing $E_F = E - V_0$ the half-plateaus appear for lower V_{sd} . The reason is that when many subbands become occupied, the simple saddle-point potential gets modified, because of charge accumulation in the channel region. To account for this, Frost *et al.*⁴ have extended the Büttiker model. They modeled the effect of charge accumulation by an explicit widening of the channel in the y direction to get the potential

$$V(x, y) = V_0 - \frac{1}{2} m^* \omega_x^2 x^2 + \frac{1}{2} m^* \omega_y^2 (|y| - W/2)^2 \quad (17)$$

for $|y| > W/2$ and

$$V(x, y) = V_0 - \frac{1}{2} m^* \omega_x^2 x^2 \quad (18)$$

elsewhere, i.e., an equipotential region in the middle of the harmonic-oscillator potential. For a small number of electrons the width $W \rightarrow 0$ and the saddle-point potential is recovered. For a larger amount of electrons the flat region widens and the subband energies become¹⁷

$$E_n = \{ -(\omega_y W/2\pi)(2m^*)^{1/2} + [\hbar\omega_y(n + \frac{1}{2}) + 2m^*(\omega_y W/2\pi)^2]^{1/2} \}^2. \quad (19)$$

The width is fitted with the experimental results in such a way that W increases with $E - V_0$ and has increasing slope ($W'' \geq 0$). A good fit in the range of interest is

$$W \propto (q_{\text{eff}} - 2)^2, \quad q_{\text{eff}} > 2, \\ W = 0, \quad q_{\text{eff}} \leq 2, \quad (20)$$

where

$$q_{\text{eff}} = \frac{E_F - eV_{\text{max}} + F(V_{sd})}{\hbar\omega_x}. \quad (21)$$

V_{max} is the maximum value of the total potential, and $F(V_{sd})$ is an increasing function of the applied potential. These effects have been added since the number of electrons through the potential decreases when the maximum value of the potential increases, and the number increases when the potential drop is higher. The two terms compensate each other partially. For the function we have used a model where F is proportional to $(V_{sd})^2$ for small voltages and linear for higher voltages, to take best account for the experimental results.

VII. COMPARISON WITH EXPERIMENT

The application of the model with the approximations described above results in a calculated differential conductance in good agreement with corresponding experiments. In the calculations the width used is according to Eq. (20) with proportionality constant equal to 5.9 and

$$F(V_{sd}) = \begin{cases} (20 \text{ V}^{-1})eV_{sd}^2, & V_{sd} \leq 7.5 \text{ mV} \\ 0.3(eV_{sd} - 3.75 \text{ meV}), & V_{sd} > 7.5 \text{ mV} \end{cases}, \quad (22)$$

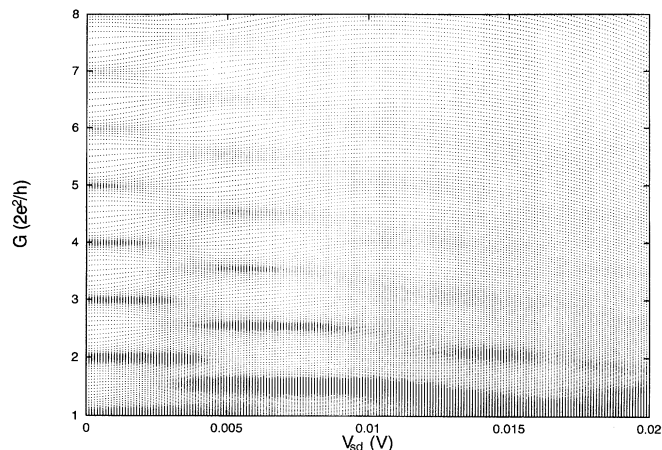


FIG. 4. Theoretical calculations of the differential conductance G vs V_{sd} for $(E - V_0)/\hbar\omega_x$ ranging from 1 to 8, $m^* = 0.067m_e$, $\hbar\omega_x = 4.5$ meV, $\hbar\omega_y = 9$ meV, $l = 50$ nm, and $\beta = 0.55$.

and the temperature is $T = V_{sd} 1000$ K/V. The chemical potential $\mu \approx E_F$ for our values of E_F and T . The conductance resulting from these calculations is displayed in Fig. 4. As can be seen the conductance plateaus for $V_{sd} = 0$ are exactly in steps of $2e^2/h$ as in the Büttiker model.¹¹ Half-plateaus occur for small V_{sd} . When E_F is higher they occur for smaller bias due to the increasing channel width. This is the same result as in the model used by Frost *et al.*,⁴ but the next line of plateaus is very diffuse, and no tendency of more plateaus can be seen. This effect is due both to the linear potential drop and the temperature dependence. When the voltage is increased to approximately 10 mV the conductance is increased,

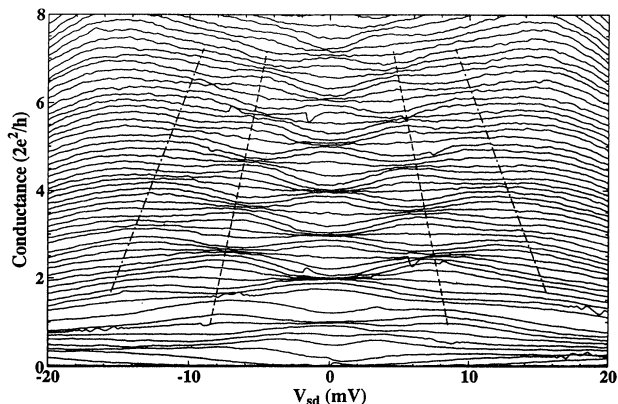


FIG. 5. Experimental differential conductance vs V_{sd} for incremental gate voltage $V_g = -0.7$ to -1.2 V with a -0.01 -V step. Taken from Ref. 4.

especially for high Fermi energies. This raising occurs since the channel width increases when the applied voltage is raised according to $F(V_{sd})$. The effect caused by raised voltage is overtaken by the effects of increasing temperature, the linear potential drop, and higher maximum value V_{max} of the total potential for even higher V_{sd} . The conductance drops and the conductance lines become parallel with each other. The experimental result (Fig. 5) measuring the conductance shows the same qualitative phenomena as the theoretical calculation.

ACKNOWLEDGMENTS

We would like to thank P. E. Lindeløf and Z.-L. Ji for informative discussions, and the Science and Engineering Research Councils of Sweden for financial support.

¹D. A. Wharam, T. J. Thornton, R. Newbury, M. Pepper, and H. Ahmed, *J. Phys. C* **21**, L209 (1988).

²B. J. van Wees, H. van Houten, C. W. J. Beenakker, J. G. Williamson, L. P. Kouwenhoven, D. van der Marel, and C. T. Foxon, *Phys. Rev. Lett.* **60**, 848 (1988).

³L. Martin-Moreno, J. T. Nicholls, N. K. Patel, and M. Pepper, *J. Phys. Condens. Matter* **4**, 1323 (1992).

⁴J. E. F. Frost, K.-F. Berggren, M. Pepper, M. Grimshaw, D. A. Ritchie, A. C. Churchill, and G. A. C. Jones, *Phys. Rev. B* **49**, 11 500 (1994).

⁵N. K. Patel, J. T. Nicholls, L. Martin-Moreno, M. Pepper, J. E. F. Frost, D. A. Ritchie, and G. A. C. Jones, *Phys. Rev. B* **44**, 13 549 (1991).

⁶Hongqi Xu, *Phys. Rev. B* **47**, 15 630 (1993).

⁷T. Heinzel, D. A. Wharam, F. M. de Aguiar, J. P. Kotthaus, G. Böhm, W. Klein, G. Tränkle, and G. Weimann, *Semicond. Sci. Technol.* **9**, 1220 (1994).

⁸F. A. Maaß, I. V. Zozulenko, and E. H. Hauge, *Phys. Rev. B* **50**, 17 320 (1994).

⁹R. Taboryski, A. K. Geim, M. Persson, and P. E. Lindelof, *Phys. Rev. B* **49**, 7813 (1994).

¹⁰M. L. Roukes *et al.*, in *Science and Engineering of 1- and 0-Dimensional Semiconductors*, edited by S. P. Beaumont and C. M. Sotomayor-Torres (Plenum, New York, 1989).

¹¹M. Büttiker, *Phys. Rev. B* **41**, 7906 (1990).

¹²D. L. Hill and J. A. Wheeler, *Phys. Rev.* **89**, 1102 (1953).

¹³S. Bjørnholm and J. E. Lynn, *Rev. Mod. Phys.* **52**, 725 (1980).

¹⁴M. J. Kelly, *J. Phys. Condens. Matter* **1**, 7643 (1989).

¹⁵M. Abramowitz and I. A. Stegun, *Handbook of Mathematical Functions* (Dover, New York, 1968).

¹⁶R. Taboryski, A. Kristensen, C. B. Sørensen, and P. E. Lindelof, *Phys. Rev. B* **51**, 2282 (1995).

¹⁷D. A. Poole, M. Pepper, K.-F. Berggren, G. Hill, and H. W. Myron, *J. Phys. C* **15**, L21 (1982).